Tuijin Jishu/Journal of Propulsion Technology
ISSN: 1001-4055
Vol. 44 No. 5 (2023)

Low Temperature Thermal Power Concept Case Study

[1]Freddie L. Inambao, [2]Shadreck M. Situmbeko

[1][2] Department of Mechanical Engineering,
University of Kwa-Zulu Natal, Durban 4000, South Africa

[1]https://orcid.org/0000-0001-9922-5434
[1] https://www.scopus.com/authid/detail.uri?authorId=55596483700

Abstract: Conventional thermal based electrical generating systems utilise high temperature heat energy to generate steam that is in turn used to drive a steam turbine. About 80% of electrical energy used in the world is produced from high temperature heat using a thermodynamic cycle known as the Rankine cycle [website en.wikipedia.org 2013]. In a Rankine cycle heat is applied externally to a closed cycle; water is normally used as the working fluid; typical temperatures are in the above 500ºC range. The usual energy sources are fossil fuels (coal, oil and natural gas), nuclear, biomass and landfill gas, and concentrated solar thermal. However, there is abundant untapped low temperature thermal resources in the form of geothermal, non-concentrated solar radiation, oceanic thermal and process industries waste heat considered not suitable for conventional thermal power plants. Low temperature energy conversion cycles are to a larger extent still a subject of research. Examples of such cycles include Organic Rankine Cycle, Kalina Cycle and Variable Phase Cycle. In this study we present an ORC concept plant based on non- concentrated solar thermal. We also explore several working fluids. Computer simulated results are presented for the proposed non-concentrated solar thermal conversion plant.

Keywords Organic Rankine Cycle, Low Temperature Thermal, Working Fluid, Non-Concentrated Solar Thermal, Computer Simulated.

1. Introduction

Low temperature energy sources include geothermal, solar thermal, oceanic thermal and process industries waste heat; figure 1 is a map showing global solar radiation resources whilst table 1 shows world geothermal resources.

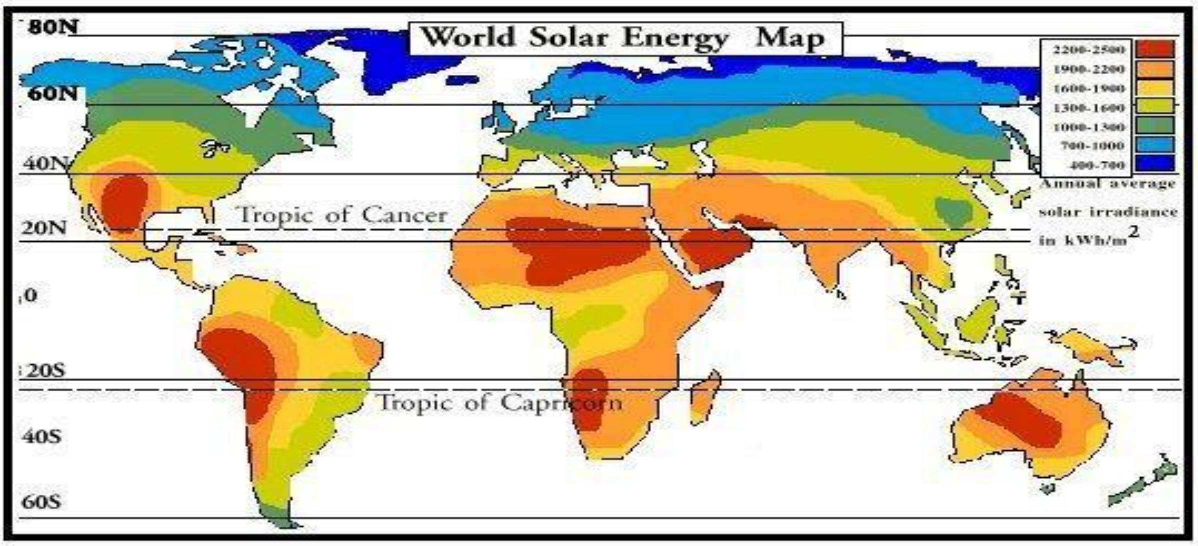

Tuijin Jishu/Journal of Propulsion Technology
ISSN: 1001-4055
Vol. 44 No. 5 (2023)

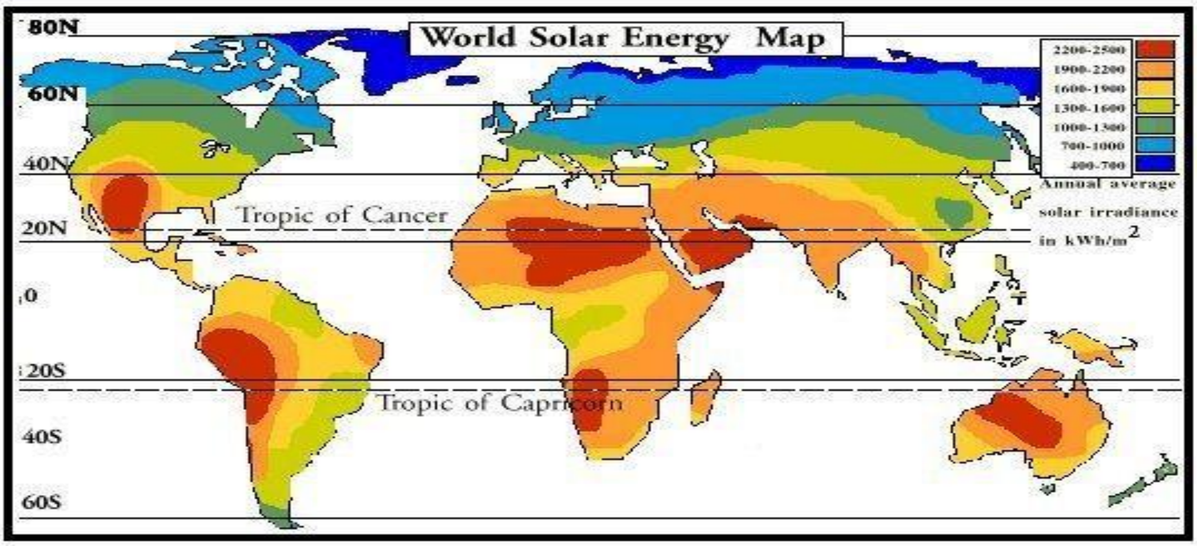

Figure 1. Global Solar Radiation Resource [website: [website: lternative-energy-resources.net (2008)]

Table 1: Global Geothermal Resources [website: geothermal-energy.org (2013)]

Region	High-temperature resources suitable for electricity generation		Low-temperature resources suitable for direct use in million TJ/yr. of heat (lower limit)
	Conventional technology in TWh/yr. of electricity	Conventional and binary technology in TWh/yr. of electricity	
Europe	1830	3700	> 370
Asia	2970	5900	> 320
Africa	1220	2400	> 240
North America	1330	2700	> 120
Latin America	2800	5600	> 240
Oceania	1050	2100	> 110
World potential	11 200	22 400	> 1400

The extent of available global oceanic energy can be inferred from the fact that oceans cover more than 70% of the earth's surface, making them the world's largest solar collectors [website: renewableenergyworld.com (2013)]. The energy potential of the oceans may be used as thermal energy due to the temperature gradient from the surface to the larger depths or as mechanical energy from the tides and waves.

Waste heat is another low temperature thermal source and is normally a by-product of many industrial processes including thermal power stations and transportation technologies such as automobiles, locomotives, ships and aircrafts. Such waste heat normally must be disposed of to the atmosphere or to a naturally occurring water body such as a lake, river or sea. Harnessing such waste heat can improve thermal efficiencies of such industrial processes and yield cost savings and optimization of operational scales.

Low temperature solar thermal energy refers to temperatures typically in the below 300ºC range. The figure below shows different temperature ranges for solar thermal energy from low to high temperature.

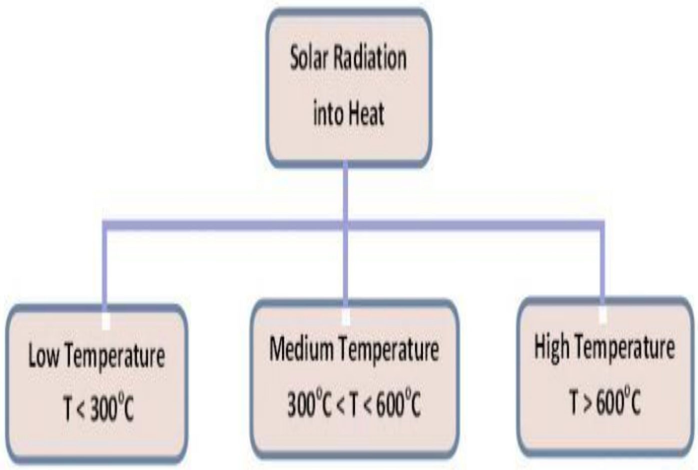

Figure 2. Solar Thermal Energy Temperature Ranges

Collection and concentration, where applicable, of solar radiation is achieved by using a solar collector system: conversion of solar radiation to heat energy and its transference to a heat transfer fluid is accomplished by an absorber or receiver. The heat transfer fluid passes its heat to a working fluid in a thermodynamic cycle via a heat exchanger. The thermodynamic cycle subsequently converts the heat energy to mechanical energy (work) in a turbine; a generator coupled to this turbine further converts the mechanical energy to electrical energy. Low concentration ratios or no concentration at all yields low temperature solar thermal. Although use of low temperature solar thermal energy, such as with flat plate and evacuated tube collectors, for power generation gives lower energy conversion efficiencies it has the benefits of simplicity of design layout, and low operation and maintenance costs; its application can normally be justified in that it takes advantage of availability of cost effective large solar collecting surfaces such as in low densely populated semi-arid and arid areas as well as oceanic areas. This situation is also more suited for power generation in remote locations as well as for distributed grid connected power in that electricity is produced nearer to the point of consumption thus reducing transportation costs and losses.

Several low temperature energy conversion technologies have been researched and continue to be an active area of research. Developed technologies include the Organic Rankine Cycle (ORC), the Kalina Cycle and the Variable Phase Cycle.

The efficiency of a heat engine is constrained by the maximum possible efficiency of an ideal cycle known as the Carnot cycle; this constraint is dependent on the temperature difference between the heat source and the heat sink and is given by the second law of thermodynamics. The figure below is a p-v diagram of the Carnot cycle. [website: optimiz.edu (2013)]

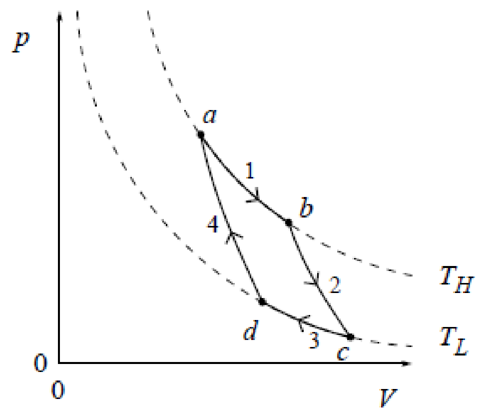

Figure 3. P-V diagram of the Carnot Cycle.

The efficiency of the Carnot cycle is given by:

$$\eta_{Carnot} = (TH-TL)/TH \qquad (1)$$

where:

η_{carnot}	:Carnot efficiency
T_H	:high temperature energy reservoir
T_L	:low temperature energy sink

Given limitations imposed by the Carnot efficiency the challenge is to optimize cycle efficiency based on other aspects. It is necessary to optimize thermal losses through appropriate geometrical design and material selection for the insulation, glazing and absorber; also, through reduction of frictional losses in the piping and optimization of working and heat transfer fluids matching with working temperature ranges.

The Organic Rankine Cycle (ORC) is in every sense the same as the conventional Rankine Cycle save for the fact that an organic fluid or a refrigerant is employed as a working fluid in place of water and steam. This allows use of low temperature heat sources such as non-concentrated solar thermal, low temperature geothermal, oceanic thermal and waste heat to generate a low temperature vapour that in turn drives a vapour turbine. This is the cycle used in this research. Figure 4 shows the ORC configuration for a geothermal application.

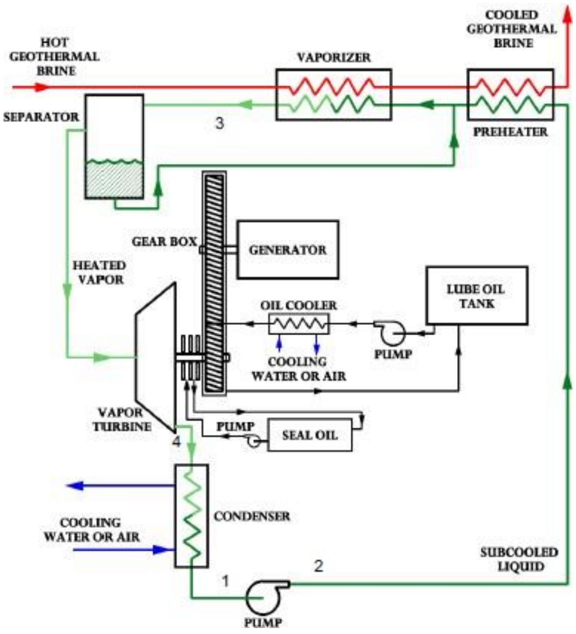

Figure 4. Organic Rankine Cycle [Geothermal_Resources_Council_2009_Poster]

2. Methodology

2.1 Solar Field Design

A solar field is initially proposed on the estimated power output of 10kW as shown in Figures 5 and 6.

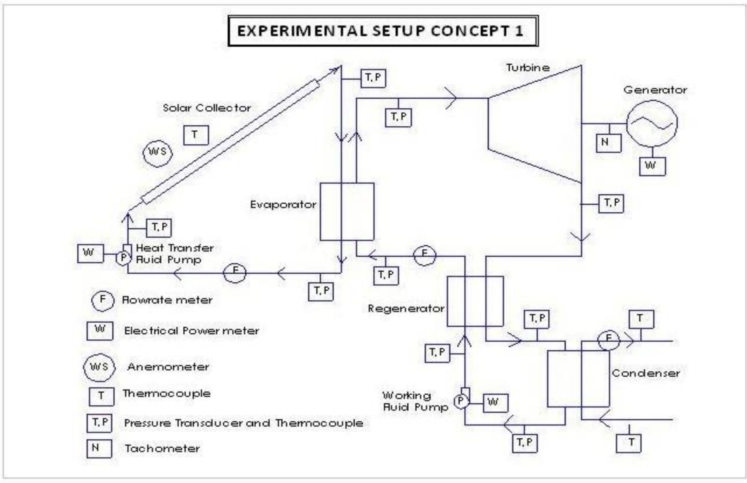

Figure 5. Concept Plant Setup for Solar Thermal ORC

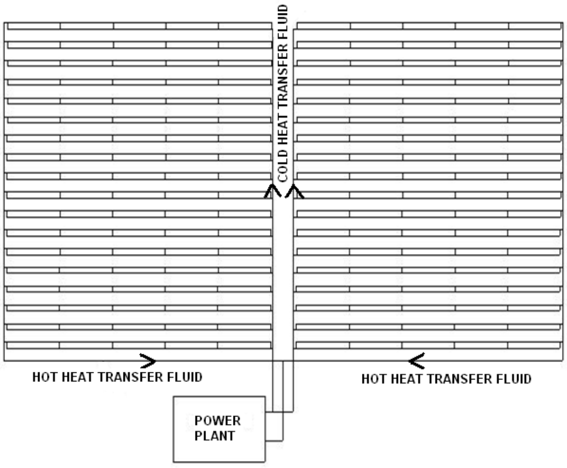

Figure 6. Proposed 10kWp Solar Field for ORC

Developing a detailed mathematical model of a solar collector requires knowledge of the geometrical measurements, and optical and thermal properties of materials used in the construction. The process is based on carrying out an energy balance which maybe steady state or transient. A transient model is more useful when the solar data can be measured and fed synchronously to the simulation model. A segmented model technique has been adopted in this study and an EES code written to establish the temperature profiles as well as thermal performance of the collector.

The figure shows the cross-section of a solar thermal collector with heat transfer balances for each component.

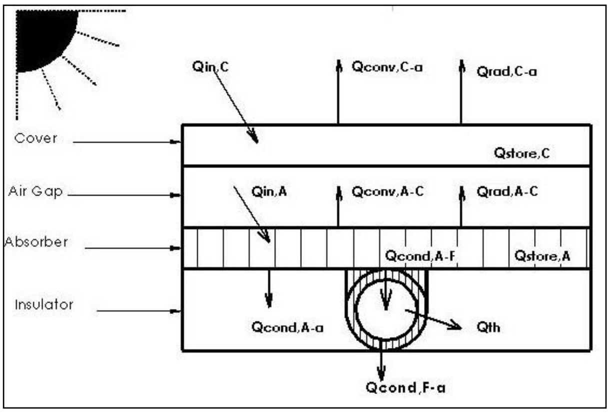

Figure 7. Solar Collector Heat Balance Layout

for the glass cover

$$Q_{store,C} = Q_{in,C} - Q_{conv,C\rightarrow a} - Q_{rad,C\rightarrow a} + Q_{conv,A\rightarrow C} + Q_{rad,A\rightarrow C} \quad (2)$$

for the absorber plate

$$Q_{store,A} = Q_{in,A} - Q_{conv,A\rightarrow C} - Q_{rad,A\rightarrow C} - Q_{cond,A\rightarrow F} - Q_{cond,A-a} \quad (3)$$

for the heat transfer fluid

$$Q_{cond,A\rightarrow F} = Q_{cond,F\rightarrow a} + Q_{th} \quad (4)$$

Tuijin Jishu/Journal of Propulsion Technology
ISSN: 1001-4055
Vol. 44 No. 5 (2023)

For the storage tank $$Q_{store,T} = Q_{th} - Q_{cond,T\to a} \qquad (5)$$

thermal efficiency $$\eta_{th} = \frac{\int Q_{th} dt}{A_c \int G dt} \qquad (6)$$

2.2 ORC Optimization

Three ORC configurations are possible based on the working fluids' Temperature-Entropy (T-s) diagrams as follows:

- conventional Rankine cycle,
- Rankine cycle with a recuperator and
- Rankine cycle with a superheater

To develop a generalized model that can be simulated using a computer program, a common configuration is indicated here from which the three models are generated:

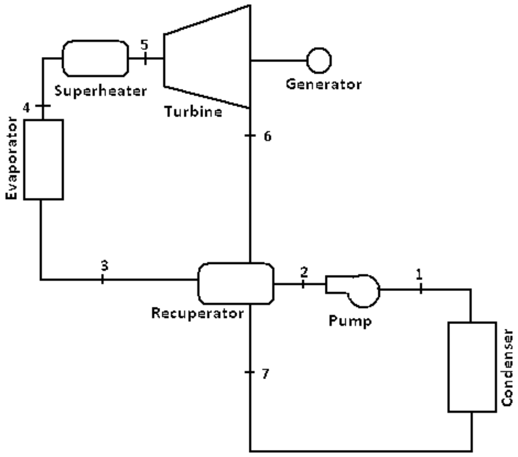

Figure 8. Common Configuration of the Organic Rankine Cycle

The mathematical models of the cycle components are given by:

Pump: $$\frac{W_{pump}}{\dot{m}} = (h_2 - h_1) \approx \frac{1\Delta P}{\eta_{pump}} \approx \frac{P_2 - P_1}{\eta_{pump}} \qquad (7)$$

Turbine: $$\frac{W_{turbine}}{\dot{m}} = (h_5 - h_6) = (h_5 - h_{6s}) \text{ x } \eta_{turbine} \qquad (8)$$

Evaporator: $$\frac{Q_{evap}}{\dot{m}} = (h_4 - h_3) \tag{9}$$

Condenser: $$\frac{Q_{cond}}{\dot{m}} = (h_7 - h_1) \tag{10}$$

Recuperator cold stream: $$\frac{Q_{recu}}{\dot{m}} = (h_3 - h_2) \tag{11}$$

Recuperator hot stream: $$\frac{Q_{recu}}{\dot{m}} = (h_6 - h_7) \tag{12}$$

Superheater: $$\frac{Q_{superheater}}{\dot{m}} = (h_5 - h_4) \tag{13}$$

Thermal efficiency: $$\eta_{therm} = \frac{W_{turbine} - W_{pump}}{Q_{in}} \approx \frac{W_{turbine}}{Q_{in}} \tag{14}$$

Where $$Q_{in} = Q_{evap} + Q_{superheater} \tag{15}$$

and in cases where there is no superheating as simply

$$\dot{Q}_{in} = \dot{Q}_{evap} \tag{16}$$

When implementing the model on the computer model an optimization scheme is included that equates either the superheating or the recuperating process or both to zero depending on the expansion characteristics of the working fluid. The optimization scheme is presented mathematically below.

If $$(s_{high} - s_{low}) / s_{low}] < \delta \tag{17}$$

then the Isentropic Curve Model is selected; otherwise,

$$If\ s_{high} > s_{low} \tag{18}$$

then the Positive Saturation Curve Model is selected; or

$$If\ s_{low} > s_{high} \tag{19}$$

then the Negative Saturation Curve Model is selected.

where s_{low} and s_{high} are the entropies of the dry saturated working fluid at the lower and higher cycle pressures respectively, and the value of the deviation δ is such that its limit approaches zero; mathematically δ→0 and in the computer model a smaller acceptable value such as 5% is assigned δ.

2.3 Solar Irradiance Modelling

Several methods have been developed including Linear Models, Polynomial Models, Angular Models, and Other Models [Koray Ulgen & Arif Hepbasli (2004)]. The method used here is based on the Angular Models as proposed by Duffie J.A. and Beckman W.A. (1991).

The total hourly radiation can be estimated from the average daily radiation by using the following equation:

$$I = Hr_t \qquad (20)$$

The coefficient to convert total daily radiation to total hourly radiation is given by:

$$r_t = \pi/24\ (a+b\cos w)\ (\cos w - \cos ws\ )/\mathrm{Sin}\,ws - (\pi ws/180)\cos ws \qquad (21)$$

Where w is the hour angle and W_s is the sunset hour angle in degrees. The coefficients a and b are given by:

$$a = 0.409 + 0.5016 \sin\,(w_S - 60) \qquad (22)$$
$$b = 0.6609 - 0.4767 sin\ (w_S - 60)$$

3. Results

Chart 1 shows results for the 180 solar collector single-pipe field model. The solar field shown in figure 6 consists of two solar banks; each solar bank consists of 18 solar arrays; and each array consists of 5 solar collectors. The computer model consists of 18 one-pipe models connected in series to represent the 180 solar collector field. There is a steady build-up of temperature for all components along the model segments and banks. The temperature is highest in the absorber plate and lowest in the transparent cover; also, the rate of temperature increase is lowest in the transparent cover. The rate of temperature increase closely follows the same profile in both the absorber and in the working fluid.

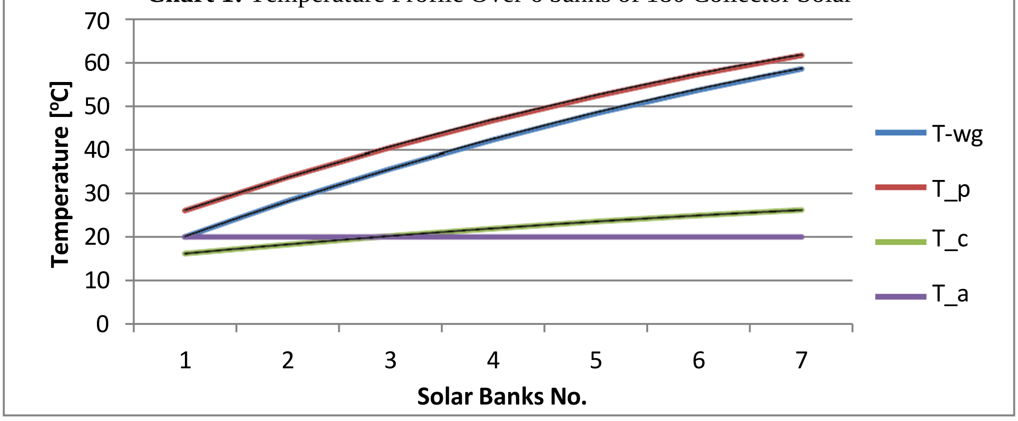

Chart 1: Temperature Profile Over 6 banks of 180 Collector Solar

Chart 2 shows the hourly temperature profiles. These simulations consist of several cycles (114 cycles calculated) to make an hour. The temperature measurement is taken at the end of the hour. These simulations include a thermal storage represented by the tank temperature. The absorber plate attains the highest temperature followed by the working fluid (water ethylene glycol) at the exit of the solar field and into the tank storage. The three temperature profiles follow each other closely and build-up slowly from morning to a high about noon. The absorber Increases temperature from ambient temperature of 20ºC to slightly over 100ºC about noon; the water ethylene glycol attains maxima of slightly below 100ºC and about 90ºC at the exit of the solar collector and in the storage tank respectively. This is desirable for heat transfer to continue flowing from the absorber to the working fluid. The transparent cover has a much lower temperature ranging from ambient temperature to about 40Cº. This ensures lower thermal losses.

Chart 2: Hourly Temperature

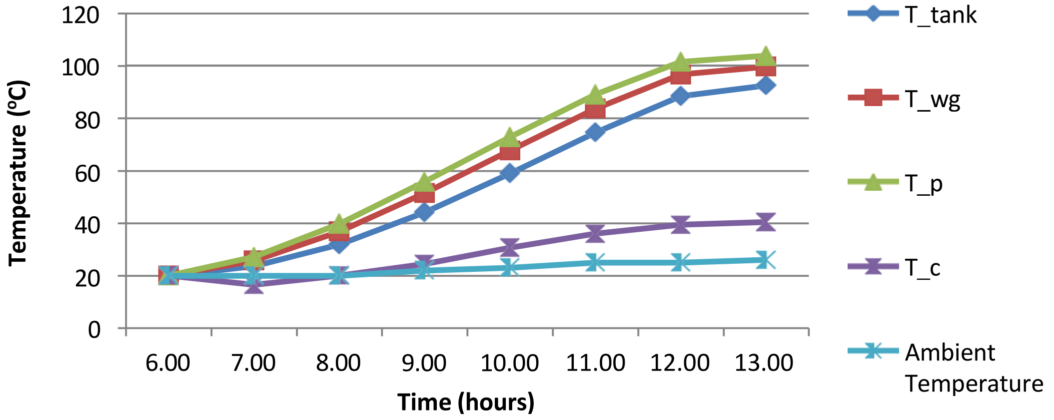

Summarized results from the ORC computer simulations are shown in the following Table 2.

Table 2 ORC Computer Simulations Results

Working Fluid	**Model Type**	**Low Temp [T_{low}]**	**High Temp [T_{high}]**	**Carnot Efficiency [ηtherm]**	**Thermal Efficiency [ηtherm]**	**Low Pressure Entropy [s_{low}]**	**High Pressure Entropy [s_{high}]**
		[C]	**[C]**	[%]	[%]	**[kJ/kg·K]**	**[kJ/kg·K]**
Benzene	ORC with No Recuperator and No Superheater	80.07	142.7	15.06	11.11	1.176	1.151
n-butane	ORC with No Recuperator and No Superheater	-0.521	50.26	15.70	11.6	2.473	2.439
n-hexane	ORC with Recuperator; No Superheater	69.28	131.3	15.33	12.1	1.462	1.44
n-pentane	ORC with Recuperator; No Superheater	35.87	92.74	15.54	12.04	1.361	1.334
Isobutane	ORC with No Recuperator and No Superheater	-11.67	37.74	15.89	11.72	2.355	2.321
Isopentane	ORC with Recuperator; No Superheater	27.86	83.77	15.66	12.2	-0.4098	-0.4366
Toluene	ORC with Recuperator; No Superheater	110.4	178.3	15.04	11.75	1.053	1.032
R22	ORC with Superheater; No Recuperator	-40.81	29.52	23.24	12.01	1.849	1.825
R113	ORC with Recuperator; No Superheater	47.61	105.7	15.33	11.89	0.7788	0.7684
R123	ORC with No Recuperator and No Superheater	27.79	80.82	14.98	11.02	1.698	1.685

R134a	ORC with Superheater; No Recuperator	-26.09	24.08	16.88	10.99	0.9712	0.9516
R141b	ORC with No Recuperator and No Superheater	32.07	86.89	15.23	11.3	1.036	1.019
R245fa	ORC with No Recuperator and No Superheater	15.19	62.85	14.18	10.38	1.784	1.77
Water	ORC with Superheater; No Recuperator	99.97	271.8	31.53	10.81	7.483	7.355

The final choice of a working fluid will be influenced apart from the thermal performance indicated in Table 2 by other factors including thermophysical properties, meeting environmental regulations and cost.

In terms of thermophysical properties an ideal working fluid should have "favorable thermodynamic properties, non-corrosive to mechanical components and safe (including nontoxic, non-flammable and environmentally benign). The desired thermodynamic properties are a boiling point somewhat below the target.

Temperature, a high heat of vaporization, a moderate density in liquid form, a relatively high density in gaseous form, and a high critical temperature." [website: optimizat.org. (2013)]. Table 3 lists the melting and boiling temperatures as well as the critical points (temperature and pressure) of the candidate working fluids. Table 4 lists the Global Warming Potential (GWP) and the Ozone Depletion Potential (ODP) of the working fluids. The GWP and ODP must also be considered in the selection of the working fluids.

Table 3 Comparison of Working Fluids Thermal Properties and ORC Thermal Requirements

Working Fluid	**Melting Temp**	**Boiling Temp**	**Critical Temp**	**Critical Pressure**
	[ºC]	**[ºC]**	**[ºC]**	**[Mpa]**
Benzene	5.5	80	289	4.74
n-butane	-138	-0.5	152	3.796
n-hexane	-95	69	234.5	3.02
n-pentane	-130	36	196.7	3.36
Isobutane	-133 to -33	-12	134.6	3.65
Isopentane	-160	28	187.25	3.38
Toluene	−95	111	318.64	4.109
R22	-175.42	-41	96.2	4.936
R113	-35	48	214.1	3.39
R123	-107	28	183.8	3.66
R134a	-103.3	-26	101.06	4.059
R141b	-103.5	32	204.15	4.25
R245fa		15.3	154.05	3.65

Table 4 Global Warming Potential and Ozone Depletion Potential of Working Fluids

Working Fluid	**Molecular Formula**	**Global Warming Potential over 100 Years (GWP~100)**	**Ozone Depletion Potential (ODP)**
Benzene	C_6H_6	0	0
n-butane	C_4H_{10}	20	0
n-hexane	C_6H_{14}	20	0
n-pentane	C_5H_{12}	11	0
Isobutane	C_4H_{10}	20	0
Isopentane	C_5H_{12}	11	0
Toluene	C_7H_8	2.7	0
R22	$CHClF_2$	1500	0.05
R113	$C_2Cl_3F_3$	6000	0.8
R123	C2HCl2F3	90	0.02
R134a	CH_2FCF_3	1300	0
R141b	C2H3Cl2F	0.09	0.11
R245fa	$C_3H_3F_5$	820	0

Ozone Depletion Potential: Reference is R11 (i.e. ODP for R11=1) Global Warming Potential: Reference is CO_2 (i.e. GWP for CO_2=1)

4. Conclusions

The paper has explored the feasibility of tapping low temperature thermal energy for generation of power based on non-concentrated solar collecting system and the organic Rankine cycle. A concept plant has been proposed and computer simulations for both the solar field and the thermal cycle have been developed on its basis.

From two models the following can be inferred: temperatures attained in the solar field model storage reached a high of about 90ºC; that means temperature T[5] in the ORC model is constrained to below this temperature.

From the ORC optimization model, it has been shown that potential working fluids and cycle configurations can be attained. Particularly in terms of performance on all accounts other than cost (and safety), the optimal working fluids are Isopentane, n-hexane, n-pentane, R141b and Benzene; when the simplicity of cycle configuration (based on the T-s diagrams) is considered Benzene and R141b perform the best.

References

[1] http://en.wikipedia.org/wiki/Electricity_generati on accessed July 4, 2013
[2] http://www.earthlyissues.com/images/0013energ ysol.jpg accessed June 14, 2013
[3] http://www.geothermal- energy.org/geothermal energy/what_is_geothe rmal_energy.html accessed July 4, 2013
[4] http://www.renewableenergyworld.com/rea/tech/ ocean-energy accessed June 14, 2013
[5] Shuba V. Raghavan etal. (2010) Chapter 6: Solar Thermal Applications, In: *Harnessing Solar Energy-Options for India*. Editors: Payal Dhar and Radha HS. Center for Study of Science, Technology and Policy (CSTEP), Bangalore, India, pp. 91-102.
[6] http://www.oberlin.edu/physics/dstyer/P111/Car not.pdf accessed June 14, 2013
[7] http://www.findthatdoc.com/search-66008087- hPDF/download-documents-geothermal- resources-council-2009-poster-pdf.htm accessed July 4, 2013
[8] Koray Ulgen & Arif Hepbasli (2004): *Solar Radiation Models. Part 2: Comparison and Developing*

New Models, Energy Sources, 26:5, 521-530

[9] Duffie J.A., Beckman W.A., 1991: *Solar Engineering of Thermal Processes*, 2nd Ed., John Wiley & Son, Inc., USA, ISBN 0-471- 51056-4

[10] http://en.wikipedia.org/wiki/Refrigerant accessed July 14, 2013

[11] http://www.engineeringtoolbox.com/Refrigeran ts-Environment-Properties-d_1220.html accessed July 17, 2013

[12] http://www.inventec.dehon.com/documents/pdf

[13] /cbac1510bfe289ca8669fe2fac5691f6.pdf accessed July 17, 2013

[14] http://www.inventec.dehon.com/documents/pdf

[15] /a7532692d1e9257a2949c15e65311b7c.pdf accessed July 17, 2013

[16] http://www.inventec.dehon.com/documents/pdf

[17] /98c2926bb0802baf7716d316ea8eed25.pdf accessed July 17, 2013

[18] http://www.hc-sc.gc.ca/ewh- semt/pubs/contaminants/psl1- lsp1/benzene/index-eng.php accessed July 17, 2013